RAPID COMMUNICATIONS

PHYSICAL REVIEW C VOLUME 47, NUMBER 4 APRIL 1993

Quasielastic scattering of ^{11}Li using realistic three-body wave functions

I. J. Thompson, J. S. Al-Khalili, and J. A. Tostevin
Department of Physics, University of Surrey, Guildford GU2 5XH, United Kingdom

J. M. Bang
The Niels Bohr Institute, DK-2100 Copenhagen Ø, Denmark
(Received 25 November 1992)

The quasielastic scattering of ^{11}Li from ^{12}C at 60 MeV/nucleon is calculated in a four-body Glauber approximation. Different ^{11}Li ground-state wave functions are used, including those calculated using Faddeev three-body models. The calculated quasielastic cross sections, including the 2^+ and 3^- states of ^{12}C in a distorted wave Born approximation, reproduce the experimental data over most of the angular range, the differences between theoretical models being less than the quoted statistical errors on the available data.
PACS number(s): 25.70.Bc, 27.20.+n

Recent experiments with neutron-rich radioactive nuclear beams [1–3] have suggested that nuclei such as ^{11}Li have a large neutron halo, or dilute neutron skin, which extends to large radii. Such experiments have measured not only the total reaction cross section for ^{11}Li projectiles but also the momentum distributions of the ^{9}Li or neutron fragments following the breakup of ^{11}Li at high energies. The neutron halo interpretation is supported by a number of recent theoretical calculations [4, 5] of the ^{11}Li ground state, some of which calculate the density [6] and breakup [7] distributions. These calculations, however, make rather different assumptions about the relative strength of pairing and spin-orbit forces experienced by the halo neutrons.

Recently, the quasielastic scattering of ^{11}Li from ^{12}C at 637 MeV has been measured [8]. We shall investigate whether the effect of the neutron halo is evident in this angular distribution and whether the present experimental data enable us to discriminate between alternative models for the ^{11}Li ground-state wave function.

To date most calculations of the ^{11}Li reaction process have used an optical-limit Glauber model [9], which requires a knowledge of only the single-particle density [6]. However, the particular feature of interest in ^{11}Li is the pairing correlations of the valence neutrons. These pairing correlations are included explicitly in the three-body models of ^{11}Li, and it is thus of interest to use the wave functions of these models in calculations to clarify the ^{11}Li reaction mechanism.

It is well known that with the lighter lithium isotopes, ^{6}Li and ^{7}Li, the reaction mechanisms are strongly influenced by polarization and/or breakup into the component clusters. In these cases, simple folding models based on the single-particle densities fail to generate the optical potentials needed to describe the elastic scattering angular distributions. With α-d and α-t separation energies of 1.47 and 2.46 MeV, respectively, for ^{6}Li and ^{7}Li, we know that dynamic polarizations are important [10, 11] and that the real part of the folded potential has to be multiplied by a factor of order 0.5 to fit the experimental data [12]. In ^{11}Li, with a ^{9}Li-nn separation energy of only 0.3 MeV, similar large effects should be expected.

The Glauber approximations can be used not only in the optical limit (where the free nucleon-nucleon reaction cross section is the essential input) but also in a three- or four-body model, with cluster-target optical potentials as the ingredient. These few-body Glauber models have been tested for deuteron scattering [13, 14], and have recently been extended to ^{11}Li, but only for the case of uncorrelated valence neutron wave functions [14, 15]. In this Rapid Communication, we present the results of a full four-body Glauber model that is able to include the full details of three-body model predictions for ^{11}Li. This model is thus able to include the correlations of the valence neutrons, their polarization and breakup induced by the reaction process, the excitation of any low-lying resonances, and to predict the effects of these on the ^{11}Li elastic scattering observables.

For the scattering of composite particles the Glauber approach involves an adiabatic treatment of the internal degrees of freedom of the projectile as well as a small angle treatment of the scattering. Both of these approximations are expected to hold at the energies of interest here.

Our four-body model for ^{11}Li scattering assumes a ^{9}Li+n+n+target description. A three-body (^{9}Li+n+n) wave function is used for ^{11}Li [4]. The ^{9}Li core is assumed to be a spectator to the reaction and hence its spin degree of freedom can be neglected. Given a choice of the ^{11}Li wave function and the n- and ^{9}Li-target optical potentials, the Glauber scattering amplitude can be calculated without further adjustable parameters.

Unlike the recent work by Yabana *et al.* [14] we include the recoil of the ^{9}Li core. Since our three-body wave function also takes into account the effects of correlations between the valence neutrons it cannot be factorized into a product of single-particle wave functions for each neutron.

The four-body Schrödinger equation is written

$$\{T_R + H_0 + U(\mathbf{R},\boldsymbol{\rho},\mathbf{r})\}\ \Psi(\mathbf{R},\boldsymbol{\rho},\mathbf{r}) \;=\; E\,\Psi(\mathbf{R},\boldsymbol{\rho},\mathbf{r}) \ , \tag{1}$$

where

$$U(\mathbf{R},\boldsymbol{\rho},\mathbf{r}) = U_c(\mathbf{R},\boldsymbol{\rho}) + U_{n1}(\mathbf{R},\boldsymbol{\rho},\mathbf{r}) + U_{n2}(\mathbf{R},\boldsymbol{\rho},\mathbf{r}) \ . \tag{2}$$

Here, $\mathbf{R}$, $\boldsymbol{\rho}$, and $\mathbf{r}$ are the coordinates of the ^{11}Li center-of-mass (c.m.), the ^{9}Li-nn separation and the n-n separation, respectively (see Fig. 1), T_R is the c.m. kinetic energy operator of the ^{11}Li projectile, and H_0 is its internal Hamiltonian. The core (^{9}Li)-target (U_c) and neutron-target ($U_{n1,2}$) optical potentials constitute only central terms. The treatment of the ^{9}Li-target Coulomb interaction is discussed later.

In the Glauber approximation [16] the elastic scattering amplitude is written

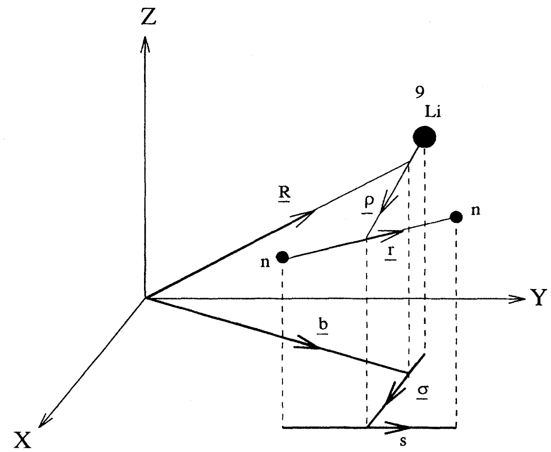

FIG. 1. Spatial coordinates of the ^{11}Li-target four-body system, and their projections on the impact parameter (X-Y) plane.

$$f_{\rm el}(\mathbf{q}) = \frac{-iK}{2\pi}\int d\mathbf{b}\ e^{i\mathbf{q}\cdot\mathbf{b}}\int d\boldsymbol{\rho}\int d\mathbf{r}|\Phi_{^{11}\rm Li}|^2\left(e^{i\chi(\mathbf{b},\boldsymbol{\sigma},\mathbf{s})}\ -\ 1\right) \ , \tag{3}$$

where the vectors $\mathbf{R}$, $\boldsymbol{\rho}$, and $\mathbf{r}$ are expressed in cylindrical polar coordinates (see Fig. 1) as $(\mathbf{b}, R_3)$, $(\boldsymbol{\sigma}, \rho_3)$, and $(\mathbf{s}, r_3)$, respectively, K is the ^{11}Li incident wave number, and $\mathbf{q}$ is the momentum transfer.

The Glauber phase shift is

$$\chi(\mathbf{b},\boldsymbol{\sigma},\mathbf{s}) = \chi_c(|\mathbf{b}_c|)\ +\ \chi_n(|\mathbf{s}_1|)\ +\ \chi_n(|\mathbf{s}_2|) \ , \tag{4}$$

with

$$\chi_c(|\mathbf{b}_c|) = -\frac{\mu}{\hbar^2 K}\int_{-\infty}^{\infty} U_c\left(\left|\mathbf{R} - \frac{2}{11}\boldsymbol{\rho}\right|\right)\ dR_3 \ , \tag{5}$$

$$\chi_n(|\mathbf{s}_i|) = -\frac{\mu}{\hbar^2 K}\int_{-\infty}^{\infty} U_n\left(\left|\mathbf{R} + \frac{9}{11}\boldsymbol{\rho} + \frac{(-1)^{i-1}}{2}\ \mathbf{r}\right|\right)\ dR_3 \ , \tag{6}$$

where the index $i = 1, 2$ labels the two neutrons and $\mathbf{b}_c$, $\mathbf{s}_1$, and $\mathbf{s}_2$ are the projections of the core and neutron coordinates (with respect to the target) on the impact parameter plane. Both the reduced mass μ and K are calculated using relativistic kinematics [17].

The ^{11}Li ground-state wave function, $\Phi_{^{11}\rm Li}$, has the general form

$$\Phi_{^{11}\rm Li}(\boldsymbol{\rho},\mathbf{r}) = \sum_{\ell\,\ell' LS} \phi_{\ell\,\ell' LS}(\rho,r)\,\{[Y_\ell(\hat\rho)Y_{\ell'}(\hat{\mathbf{r}})]_L\,[\chi_1\chi_2]_S\}_{J=0,M=0} \ , \tag{7}$$

where the χ_i are the neutron spinors. In the present calculations the wave function includes both S- and P-wave components. The angular momentum labels on the radial wave functions are hence equal ($\ell = \ell' = S = L$) and we abbreviate the notation to $\phi_L(\rho, r)$, where $L = 0, 1$.

As the Glauber phase shift $\chi(\mathbf{b},\boldsymbol{\sigma},\mathbf{s})$ is a function of vectors which lie in the impact parameter plane, the Z-component integrations in the amplitude of Eq. (3) involve only the wave function. Thus we first evaluate the ^{11}Li density projected onto the impact parameter plane (the Glauber "thickness" function),

$$\xi(\boldsymbol{\sigma},\mathbf{s}) = \int_{-\infty}^{\infty} d\rho_3\int_{-\infty}^{\infty} dr_3\ \langle|\Phi_{^{11}\rm Li}(\boldsymbol{\rho},\mathbf{r})|^2\rangle_{\rm spin} \ , \tag{8}$$

where $\langle\ \rangle_{\rm spin}$ denotes an integration over spin coordinates. From the definition of the wave function,

$$\langle|\Phi_{^{11}\rm Li}(\boldsymbol{\rho},\mathbf{r})|^2\rangle_{\rm spin} = \frac{1}{(4\pi)^2}\sum_{L,\Lambda}(-1)^{L+\Lambda}\ (2L+1)^2\ (2\Lambda+1)\ W(LLLL;L\Lambda)\begin{pmatrix} L & L & \Lambda\\ 0 & 0 & 0\end{pmatrix}^2\ P_\Lambda(\cos\gamma)\ |\phi_L(\rho,r)|^2 \ , \tag{9}$$

with $P_\Lambda(\cos\gamma)$ a Legendre polynomial and γ the angle between $\boldsymbol{\rho}$ and $\mathbf{r}$. Explicitly,

$$\cos\gamma = \frac{\rho_3 r_3}{\rho r} + \frac{\sigma s}{\rho r}\cos(\varphi_\rho - \varphi_r) , \tag{10}$$

and hence

$$\xi(\boldsymbol{\sigma},\mathbf{s}) = g_1(\sigma,s) + g_2(\sigma,s)\cos(\varphi_\rho - \varphi_r) + g_3(\sigma,s)\cos^2(\varphi_\rho - \varphi_r) , \tag{11}$$

where

$$g_1(\sigma,s) = \frac{1}{(4\pi)^2}\int_{-\infty}^{\infty} d\rho_3 \int_{-\infty}^{\infty} dr_3 \left[\phi_0^2(\rho,r) + \frac{3}{2}\left(-\left(\frac{\rho_3 r_3}{\rho r}\right)^2 + 1\right)\phi_1^2(\rho,r)\right] , \tag{12}$$

$$g_2(\sigma,s) = -\frac{3}{(4\pi)^2}\,\sigma s \int_{-\infty}^{\infty} d\rho_3 \int_{-\infty}^{\infty} dr_3\, \frac{\rho_3 r_3}{(\rho r)^2}\phi_1^2(\rho,r) , \tag{13}$$

$$g_3(\sigma,s) = -\frac{3}{2(4\pi)^2}\,(\sigma s)^2 \int_{-\infty}^{\infty} d\rho_3 \int_{-\infty}^{\infty} dr_3 \left(\frac{\phi_1(\rho,r)}{\rho r}\right)^2 . \tag{14}$$

The elastic amplitude, with $q = 2K\sin(\theta/2)$, is therefore

$$f_{\rm el}(\theta) = \frac{-iK}{2\pi}\int d\mathbf{b}\, e^{i\mathbf{q}\cdot\mathbf{b}} \int d\boldsymbol{\sigma} \int d\mathbf{s}\, \xi(\boldsymbol{\sigma},\mathbf{s}) \left(e^{i\chi(\mathbf{b},\boldsymbol{\sigma},\mathbf{s})} - 1 \right) . \tag{15}$$

In the above, the phase shift χ is due to the strong interaction only. We incorporate the Coulomb interaction of the ^{9}Li core with the target by including the contribution $\chi^a_{\rm Coul}$ from a screened Coulomb potential of screening radius a, and expanding and retaining only the leading terms [13, 18] in powers of b_c/a. We find $\chi^a_{\rm Coul}\,(b_c) = \chi_\rho(b_c) + \chi^a_s$, where

$$\chi_\rho(b_c) = \begin{cases} -2\eta(\lambda/R_{\rm Coul})[1 + \frac{1}{3}(\lambda/R_{\rm Coul})^2] + 2\eta\ln(KR_{\rm Coul} + K\lambda) , & b_c < R_{\rm Coul} , \\ +2\eta\ln Kb_c , & b_c \geq R_{\rm Coul} , \end{cases} \tag{16}$$

Z is the target charge, $R_{\rm Coul}$ its Coulomb radius, and $\chi^a_s = -2\eta\ln(2Ka)$. Here, $\lambda(b_c) = (R^2_{\rm Coul} - b^2_c)^{\frac{1}{2}}$ and $\eta = Ze^2\mu/K$ is the Sommerfeld parameter.

Upon adding the point-charge Coulomb amplitude to the Glauber amplitude [13, 18]

$$f_{\rm el}(\theta) \;=\; e^{i\chi^a_s}\left\{ f_{\rm pt}(\theta) \;-\; \frac{iK}{2\pi}\int d\mathbf{b}\, e^{i\mathbf{q}\cdot\mathbf{b}+2i\eta\ln Kb}\,\left(e^{i\chi_{\rm opt}(\mathbf{b})} - 1\right)\right\}, \tag{17}$$

where

$$e^{i\chi_{\rm opt}(\mathbf{b})} = \int d\boldsymbol{\sigma}\int d\mathbf{s}\;\xi(\boldsymbol{\sigma},\mathbf{s})\left(e^{i[\chi(\mathbf{b},\boldsymbol{\sigma},\mathbf{s}) + \chi_\rho(\mathbf{b},\boldsymbol{\sigma}) - 2\eta\ln Kb]}\right) . \tag{18}$$

The overall phase factor χ^a_s (the only effect of the screening radius) can be ignored when calculating the cross sections from this expression.

The calculation of the elastic scattering of ^{11}Li requires the specification of (i) the ^{11}Li ground-state wave function, and (ii) the neutron- and core (^{9}Li)-target optical potentials. For the neutron-target interaction, we follow [14] and use the Becchetti-Greenlees parametrization [19] appropriate to the beam energy, but without the spin-orbit force. At 637/11 MeV/nucleon, for a ^{12}C target, we therefore use

$$V = 37.4\ \text{MeV},\quad r_V = 1.20\ \text{fm},\quad a_V = 0.75\ \text{fm},$$
$$W = 10.0\ \text{MeV},\quad r_W = 1.3\ \text{fm},\quad a_W = 0.6\ \text{fm}.$$

The choice of the ^{9}Li-^{12}C interaction is more problematic. Since no ^{9}Li scattering data have been measured, we have to rely on data obtained with similar nuclei. Optical potentials for ^{12}C-^{12}C scattering have been determined at 30 and 85 MeV/nucleon [20]. We have linearly interpolated these potential parameters in energy to obtain values for use in ^{9}Li-^{12}C scattering at 637/11 (57.9) MeV/nucleon:

$$V = 147.0\ \text{MeV},\quad r_V = 0.641\ \text{fm},\quad a_V = 0.885\ \text{fm},$$
$$W = 25.0\ \text{MeV},\quad r_W = 1.012\ \text{fm},\quad a_W = 0.755\ \text{fm}.$$

The radius parameters are multiplied by $9^{1/3} + 12^{1/3}$.

Using these potential parameters, and the Faddeev three-body wave functions for ^{11}Li from [4], we have calculated the Glauber cross sections $\sigma_{\rm el}(\theta) = |f_{\rm el}(\theta)|^2$.

These cross sections are shown in Fig. 2, for different models of ^{11}Li [4]. Curve M3 uses the "spin-orbit limit" wave function with potential radius 1.1 fm, while curve Q5 uses the larger radius of 1.45 fm and gives a slightly larger ^{11}Li matter radius. In both cases, the ^{11}Li ground state is predominantly a $(0p_{1/2})^2$ configuration, moderated by pairing correlations. Curve L6A on the other hand arises from the "pairing limit" wave function, where pairing correlations are assumed to dominate a (weak) spin-orbit force in the $0p$ shell, so that the neutrons are entirely in a relative $^1S_0$ state.

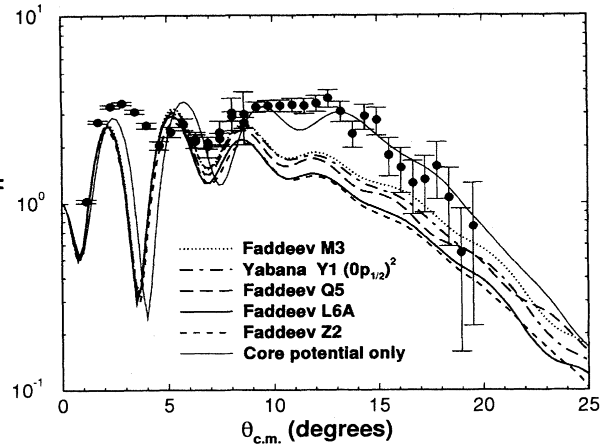

FIG. 2. Calculated ^{11}Li-^{12}C elastic scattering at 637 MeV using different three-body models for ^{11}Li, and when using the core potential only. The data are the quasielastic cross sections of [8].

We also show the predictions of the model Z2 of [21], and curve Y1 is the pure uncorrelated $(0p_{1/2})^2$ configuration as used in [14]. For comparison, the scattering due only to the core potential (with radius calculated using $9^{1/3}+12^{1/3}$) is also shown. The figure shows that, upon inclusion of the valence nucleon halo, there is considerable additional absorption for scattering angles greater than 5°, and that there is a shift in the phase of the oscillations caused by the real part of the polarization potential.

The experimental energy resolution in the data of [8] does not allow for the separation of the elastic scattering from the inelastic scattering to low-lying collective states; in particular the 2^+ and 3^- states of ^{12}C, which should make the largest contributions. These have to be calculated separately and added to the $\sigma_{\rm el}(\theta)$ calculated from the Glauber model.

In estimating these inelastic contributions we need to decide whether the distorted wave Born approximation (DWBA) or the coupled-channels approach should be used. Since ^{12}C and ^{9}Li have the same neutron number, we will assume as a first approximation that ^{12}C and ^{9}Li have similar deformed shapes, and that their inelastic processes have similar effects on the optical potential. To this extent our interpolated ^{9}Li-^{12}C optical potential, deduced from ^{12}C-^{12}C data, already includes the back-coupling effects of the ^{9}Li and ^{12}C excitation. We thus use the interpolated ^{9}Li-^{12}C potential directly in our Glauber calculations and add the ^{12}C inelastic processes in a DWBA step as follows.

To calculate the DWBA cross sections to the 2^+ and 3^- states of ^{12}C within the Glauber model, we have deformed the "Glauber optical potential"

$$U_{\rm opt}(r) = \frac{\hbar^2 K}{2\mu\pi}\frac{1}{r}\frac{d}{dr}\int_r^\infty \frac{\chi_{\rm opt}(b)}{\sqrt{b^2-r^2}} b\, db\ . \qquad (19)$$

This scheme reproduces $f_{\rm el}(\theta)$ very closely [14]. The deformed Glauber optical potential is then included in a FRESCO [22] DWBA calculation. We follow [8] and use deformation lengths of $\delta_2 = 1.648$ fm and $\delta_3 = 1.00$ fm for the ^{12}C 2^+ and 3^- states, respectively. These inelastic cross sections are now used to construct the quasielastic cross section.

Figure 3 shows the quasielastic cross sections for the different models of ^{11}Li. In this figure the higher curves are from the models with large $(0p_{1/2})^2$ configurations and give a better fit in the midangles. The models of ^{11}Li with large nn correlations lead to lower cross sections in this range. At large angles the data do not permit us to properly discriminate between the models. These conclusions could however easily be changed by adjustments to the ^{9}Li-^{12}C optical potential, estimated here from ^{12}C-^{12}C data. Clearly the measurement of ^{9}Li angular distributions will be vital to the clarification of the core-target interaction and an unambiguous understanding of the ^{11}Li reaction mechanisms.

The first calculation of ^{11}Li elastic scattering [23] made use of ^{12}C-^{12}C data to construct a ^{11}Li optical potential directly. They determined what renormalization of an M3Y double-folded potential was required to fit the ^{12}C-^{12}C data, and then applied the same factor ($N = 1.175 + 0.725i$) to a double-folded potential using ^{11}Li and ^{12}C densities. The neutron halo enters here through the diffuse tail in the ^{11}Li density. This renormalized double-folded potential was used in [8] as the bare potential for a coupled-channels calculation of the ^{12}C ground, 2^+ and 3^- states. The resulting sum of these quasielastic channels produce fits to the data [8] of comparable quality to those obtained here. However, for the reasons given above, we believe that these inelastic channels should be calculated using a DWBA rather than a coupled-channels method. Had the DWBA results for the inelastic channels been used, the quasielastic sum would have been larger by more than a factor of 2, suggesting that this approach underestimates the absorption in the core potential and/or in the reactions of the valence neutrons.

A second calculation [14] used potentials similar to ours, based on the observed ^{12}C-^{12}C energy dependence

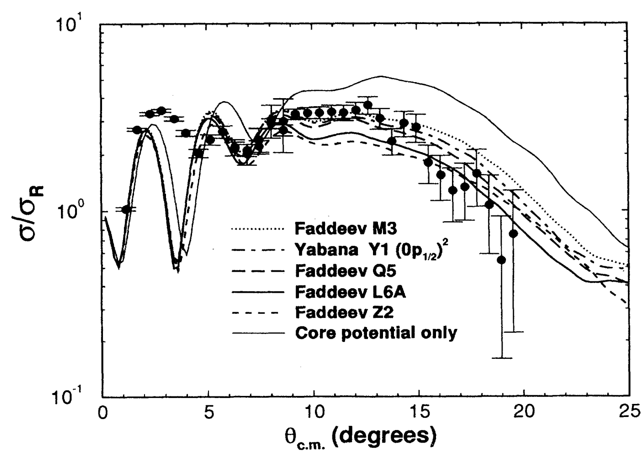

FIG. 3. Calculated ^{11}Li-^{12}C quasielastic scattering at 637 MeV from different three-body models for ^{11}Li, and when using the core potential only. The data are from [8].

[20], though for elastic scattering only and using an uncorrelated $(0p_{1/2})^2$ wave function for ^{11}Li. Their interpolation procedure, however, underestimated the radius of the imaginary potential, and predicted a cross section that must become too large with the addition of the DWBA inelastic cross sections.

A feature of all these theoretical calculations is the presence of a sharp minimum at 4° in the calculated angular distributions. This discrepancy with experiment remains unexplained.

The calculation of the elastic angular distributions is the first result of our Glauber four-body model for the reaction mechanism of ^{11}Li. We have included all the ground-state correlations in the structure of ^{11}Li given by various models, and determined their effect on the elastic and quasielastic scattering cross sections. The errors on the available data do not yet permit us to properly discriminate between the models. The general conclusion, however, is that the elastic scattering oscillations are shifted to smaller angles by the polarization effects, and that there is increased absorption for small impact parameters. Those models of ^{11}Li with large nn correlations result in lower cross sections in this angular range.

In principle, measurement of elastic angular distributions should provide a useful indicator of the nature of the ^{11}Li ground state, and help to decide between competing theoretical models of the ground-state structure. Moreover, since the Glauber four-body model provides a theoretical description of the scattering process in which all ground-state correlations can be accounted for, the coincidence breakup distributions calculated using this model should provide a sensitive probe of the nature of the neutron halo.

Support from SERC Grants No. GR/G 0109.6 and No. GR/H 2402.0 is acknowledged.

[1] I. Tanihata, H. Hamagaki, O. Hashimoto, S. Nagamiya, Y. Shida, N. Yoshikawa, O. Yamakawa, K. Sugimoto, T. Kobayashi, D.E. Greiner, N. Takahashi, and Y. Nojiri, Phys. Lett. **160B**, 380 (1985).

[2] I. Tanihata, T. Kobayashi, O. Yamakawa, T. Shimoura, K. Ekuni, K. Sugimoto, N. Takahashi, T. Shimoda, and H. Sato, Phys. Lett. B **206**, 592 (1988).

[3] W. Mittig, J.M. Chouvel, Zhan Wen Long, L. Bianchi, A. Cunsolo, B. Fernandez, A. Foti, J. Gastebois, A. Gillebert, C. Gregoire, Y. Schutz, and C. Stephan, Phys. Rev. Lett. **59**, 1889 (1987).

[4] J.M. Bang and I.J. Thompson, Phys. Lett. B **279**, 201 (1992).

[5] G.F. Bertsch, B.A. Brown, and H. Sagawa, Phys. Rev. C **39**, 1154 (1989); T. Hoshino, H. Sagawa, and A. Arima, Nucl. Phys. **A506**, 271 (1990); L. Johannsen, A.S. Jensen, and P.G. Hansen, Phys. Lett. B **244**, 357 (1990); A.C. Hayes, *ibid.* **254**, 15 (1991); M.V. Zhukov, B.V. Danilin, D.V. Fedorov, J.S. Vaagen, F.A. Gareev, and J.M. Bang, *ibid.* **265**, 19 (1991); G.F. Bertsch and H. Esbensen, Ann. Phys. **209**, 327 (1991); Y. Tosaka and Y. Suzuki, Nucl. Phys. **A512**, 46 (1990).

[6] M.V. Zhukov, D.V. Fedorov, B.V. Danilin, J.S. Vaagen, J.M. Bang, and I.J. Thompson, Nucl. Phys. A (in press).

[7] H. Esbensen, Phys. Rev. C **44**, 440 (1991); C.A. Bertulani and K.W. McVoy, Michigan State Report No. MSUCL-834, 1992; M.V. Zhukov, D.V. Fedorov, B.V. Danilin, J.S. Vaagen, and J.M. Bang, Nucl. Phys. **A539**, 177 (1992); M.V. Zhukov, B.V. Danilin, D.V. Fedorov, J.M. Bang, I.J. Thompson, and J.S. Vaagen, Phys. Rep. (in press).

[8] J.J. Kolata, M. Zahar, R. Smith, K. Lamkin, M. Belbot, R. Tighe, B.M. Sherrill, N.A. Orr, J.S. Winfield, J.A. Winger, S.J. Yennello, G.R. Satchler, and A.H. Wuosmaa, Phys. Rev. Lett. **69**, 2631 (1992).

[9] G.F. Bertsch, H. Esbensen, and A. Sustich, Phys. Rev. C **42**, 758 (1990); I. Tanihata, K. Yoshida, T. Suzuki, T. Kobayashi, S. Shimoura, K. Sugimoto, K. Matsuta, T. Minamisono, O. Testard, W. Christie, D. Olson, and H. Wieman, in *Proceedings of the Second International Conference on Radioactive Nuclear Beams*, Louvain-la-Neuve, 1991, edited by Th. Delbar (Hilger, Bristol, 1992).

[10] I.J. Thompson and M.A. Nagarajan, Phys. Lett. **106B**, 163 (1981).

[11] M.A. Nagarajan, I.J. Thompson, and R.C. Johnson, Nucl. Phys. **A385**, 525 (1982).

[12] G.R. Satchler and W.G. Love, Phys. Lett. **76B** 23 (1978).

[13] J.S. Al-Khalili and R.C. Johnson, Nucl. Phys. **A546**, 622 (1992).

[14] K. Yabana, Y. Ogawa, and Y. Suzuki, Phys. Rev. C **45**, 2909 (1992).

[15] K. Yabana, Y. Ogawa, and Y. Suzuki, Nucl. Phys. **A539**, 295 (1992).

[16] R.J. Glauber, in *Lectures in Theoretical Physics*, edited by W.E. Brittin (Interscience, New York, 1959), Vol. 1, p. 315.

[17] W.R. Coker, L. Ray, and G.W. Hoffmann, Phys. Lett. **64B**, 403 (1976).

[18] R.J. Glauber, in *Proceedings of 3rd International Conference on High Energy Physics and Nuclear Structure*, Columbia, 1969, edited by S. Devons (Plenum, New York, 1970); R.J. Glauber and G. Matthiae, Nucl. Phys. **B21**, 135 (1970).

[19] F.D. Becchetti and G.W. Greenlees, Phys. Rev. **182**, 1190 (1969).

[20] M.-E. Brandan, Phys. Rev. Lett. **60**, 784 (1988).

[21] M.V. Zhukov, B.V. Danilin, D.V. Fedorov, J.S. Vaagen, F.A. Gareev, and J.M. Bang, Phys. Lett. B **265**, 19 (1991).

[22] I.J. Thompson, Comput. Phys. Rep. **7**, 167 (1988).

[23] G.R. Satchler, K.W. McVoy, and M.S. Hussein, Nucl. Phys. **A522**, 621 (1991).